Superlattices and Microstructures xxx (2017) 1–10

Contents lists available at ScienceDirect

Superlattices and Microstructures

journal homepage: www.elsevier.com/locate/superlattices

# Mesoporous thin film structures as metal nanoparticle reactors for electronic circuits: Effects of matrix crystallinity and nanoparticle functionalization

Diana C. Delgado, Diego E. Pérez Gagni, Paolo N. Catalano**, Martín G. Bellino*

*Departamento de Micro y Nanotecnología, Instituto de Nanociencia y Nanotecnología-Comisión Nacional de Energía Atómica, CONICET, Av. General Paz 1499, B1650KNA, San Martín, Argentina*

ARTICLE INFO

*Article history:*
Received 16 March 2017
Received in revised form 2 May 2017
Accepted 3 May 2017
Available online xxx

*Keywords:*
Nanoelectronics
Mesoporous oxide thin films
Silver nanoparticles
Self-assembled monolayers

ABSTRACT

There is an increasing interest in versatile nanoelectronic structures based on stable, accessible and spatially located arrays of metal nanoparticles. In this study, the influences of mesoporous titania thin film crystallinity and pore features over electrical conductivity of embedded Ag-nanoparticles were analyzed. Although matrices treated at lower temperatures have shown less pore connectivity, less extensive anatase fraction and lower silver content, they revealed higher electrical conductivity than matrices treated at higher temperatures. This was interpreted as better connectivity among particles from plasmon behavior. The stability of this system was significantly enhanced through upon chemisorption of 1-octanethiol self-assemble monolayers over Ag-nanoparticles. The maximum plasmon absorbance remained practically unaltered after storage for at least 15 days and the current remains stable up to 20 voltage cycles. This demonstrates that a stable and accessible conductive nanocomposite circuit consisting of alkanethiol-functionalized metal nanoparticles embedded in a mesoporous oxide thin film matrix can be produced.



## 1. Introduction

There is an increasing interest in methods for fabricating versatile nanoelectronic structures based on highly controllable three-dimensional arrays of metal nanoparticles [1–3]. In fact, nowadays nanoelectronic is one of the hottest fields of nanomaterials related research, and several applications are being explored, e.g., detectors, memory chips, and fuel cells [4]. Numerous metal nanoparticle morphologies as well as several assembly methods based on lithography [5–7] or layer by layer deposition [8], have been introduced for constructing dimensionally nano architectures. In addition to their utility in nanoelectronics, there is also growing evidence that metal nanoparticles can improve the sensing properties compared to their bulk counterparts [9,10]. Furthermore, the functionality of these metal nanostructures can be modified specifically through upon chemisorption of self-assembled monolayers (SAMs) of alkanethiols bearing terminal functional groups owing to their ease of formation and affinity to metal substrates [11]. This capability is in the origin of applications such as DNA sensing [12]. However, to maximize the potential of metal nanoparticles in electronic applications, closely packed

* Corresponding author.
** Corresponding author.
*E-mail addresses:* catalano@cnea.gov.ar (P.N. Catalano), mbellino@cnea.gov.ar (M.G. Bellino).

http://dx.doi.org/10.1016/j.spmi.2017.05.002
0749-6036/

nanoparticle assembly, spatial location and hierarchical organization control are needed. Mesoporous oxide thin films (MOTF) have proved to be a very useful medium for nanotechnology development. MOTF have the inherent capabilities of highly controlled nanoreactors and thus are attractive matrices for constructing and organizing metal nanostructures [13]. Their distinctive properties are a function of the high surface area, the size and interconnectedness of the pores, and the chemical nature of the framework. Embedding metal nanoparticles within thin films permits to exploit their properties derived from size or confinement and protect them from the environment. In particular, MOTF provide grant accessibility to ions or molecules and, indeed, highly restricted chemical environments due to their controlled pore size domains, which constitute an ideal matrix for metallic nanoparticle applications. In fact, the resulting electrical properties due to metal confinement and possibility to combine the accessibility of the mesopore system and the protective properties of the matrix bring the opportunity to create synergic nanosystems. In addition, MOTF building blocks consisting of different composition and pore structure have shown to assemble into well-defined multilayers. The use of MOTF matrices has already derived to improvements in the exploitation of optical and catalytic properties of embedded metal nanoparticles leading to advances in plasmonics [14] and energy conversion [15]. Along these lines, different synthesis approaches to typically obtain these nanocomposites have been reported such as direct incorporation of preformed nanoparticles into the mesoporous materials and salt impregnation followed by reduction [13]. We have previously used mesoporous titania films to synthetize patterned silver nanoparticles arrays by a photocatalysis-assisted lithography procedure [6] and considered whether they can be used as nanoelectrodes using a conductive-tip AFM [16]. Because nanoparticles can localize on multiple layered architectures, there may be scope for designing hierarchical metal-oxide electronic nanostructures. However, metal nanoparticles embedded into mesoporous films present low and instable electrical conductivity and this has, so far, prevented their use in the design of metal nanoparticle/mesoporous film based circuitries. The vision of this work was to create actual metal nanoparticle stable electrical currents into mesoporous films. We have achieved this goal by using localized silver nanoparticles stabilized by SAMs of alkane thiols into hierarchical 3D layered $SiO_2/TiO_2/SiO_2$ mesoporous structures. The nanoparticle array is therefore accessible for any chemical or biological modification paving the way for creating novel sensors.

## 2. Experimental

### 2.1. Synthesis and deposition of mesoporous layers

Silicon (1.0.0) wafer (University Wafer, Inc., Boston, MA) pieces (2 × 2 cm) or standard microscope glass slide pieces (2 × 2.5 cm) were thoroughly rinsed with miliQ water, acetone and isopropanol, and finally dried under nitrogen flow. Silica-titania bilayer mesoporous thin films were prepared by sequential spin-coating (3100 rpm for 30 s) on the substrates. A first layer of mesoporous $SiO_2$ was deposited on the substrates. Tetraethyl orthosilicate (TEOS) (Sigma-Aldrich) was used as the inorganic precursor and Pluronics F127 ($HO(CH_2CH_2O)_{106}(CH_2CH(CH_3)O)_{70}$-$(CH_2CH_2O)_{106}OH$) (Sigma-Aldrich) was selected as the organic template. TEOS was prehydrolyzed by refluxing for 1 h in a water/ethanol solution; $[H_2O]/[Si] = 1$; $[EtOH]/[TEOS] = 5$. Surfactant, ethanol and acidic water were added to this prehydrolyzed solution in order to prepare the precursor solution with final composition TEOS:ethanol:$H_2O$ (0.1 M HCl):F127 equal to 1:40:5:0.0075 mol ratios. After deposition, the samples were placed in a 50% RH chamber for 1 h and subjected to a consolidation thermal treatment consisting of two successive stages of 30 min at 60 and 130 °C, followed by a final heat treatment at 200 °C for 2 hs. Next, a second layer of mesoporous $TiO_2$ was deposited on top of the deposited $SiO_2$ layer, obtained from a $TiCl_4$/ethanol solution to which the organic template Pluronics F127 and water were added. The final composition of the precursor solution was $TiCl_4$:ethanol:$H_2O$:F127 equal to 1:40:10:0.0075 mol ratios. The substrates were spin-coated at 35 °C solution temperature and a relative humidity (RH) of 30%. After this second deposition, the samples were introduced into a 50% RH chamber for 1 h and then thermally stabilized with two successive stages of 30 min at 60 °C and 130 °C, followed by a final heat treatment at 200 °C for 2 hs. A third mesoporous silica layer (equal composition to the first silica mesostructure) was selectively deposited by micromolding in capillaries (MIMIC) [17–19], where the silica precursor solution was filled into microgrooves defined by a polydimethylsiloxane (PDMS) cast and the surface of titania layer. After curing incubation in an ethanol chamber for 30 min the PDMS cast was removed creating rectangular ridges of 300 μm width and 500 nm height.

Finally, to stabilize the overall structure and to remove the organic template a final thermal treatment at 350 °C or 500 °C for 2 hs (temperature ramp of 2 °C/min) was performed. Two different final treatment temperatures were chosen to evaluate differential development of anatase phase within the mesoporous titania layer.

### 2.2. Selective photodeposition and thiol-modification of silver nanoparticles

Samples were immersed in a previously deoxygenated 1 M $AgNO_3$ water-ethanol solution (1:1 vol ratio) for 10 min in the dark to allow ion infiltration. Subsequently, samples were individually placed in a 60 mm plastic culture dish and 8 mL of the silver solution was added to each one so the samples were completely immersed. The dishes were placed 2 cm below a UV tube lamp (Yarlux, 15 W, emission peak at 355 nm) for 60 min under constant nitrogen flow. A mask was used for selective deposition of silver nanoparticles in a square area of 6.3 $mm^2$. Photodeposition was performed in such a way that the ridges previously fabricated by soft-lithography patterning, were located across the central zone of nanoparticles deposited area. The samples were then withdrawn from the silver solution, thoroughly rinsed with water and dried under nitrogen flow. A

Please cite this article in press as: D.C. Delgado et al., Mesoporous thin film structures as metal nanoparticle reactors for electronic circuits: Effects of matrix crystallinity and nanoparticle functionalization, Superlattices and Microstructures (2017), http://dx.doi.org/10.1016/j.spmi.2017.05.002

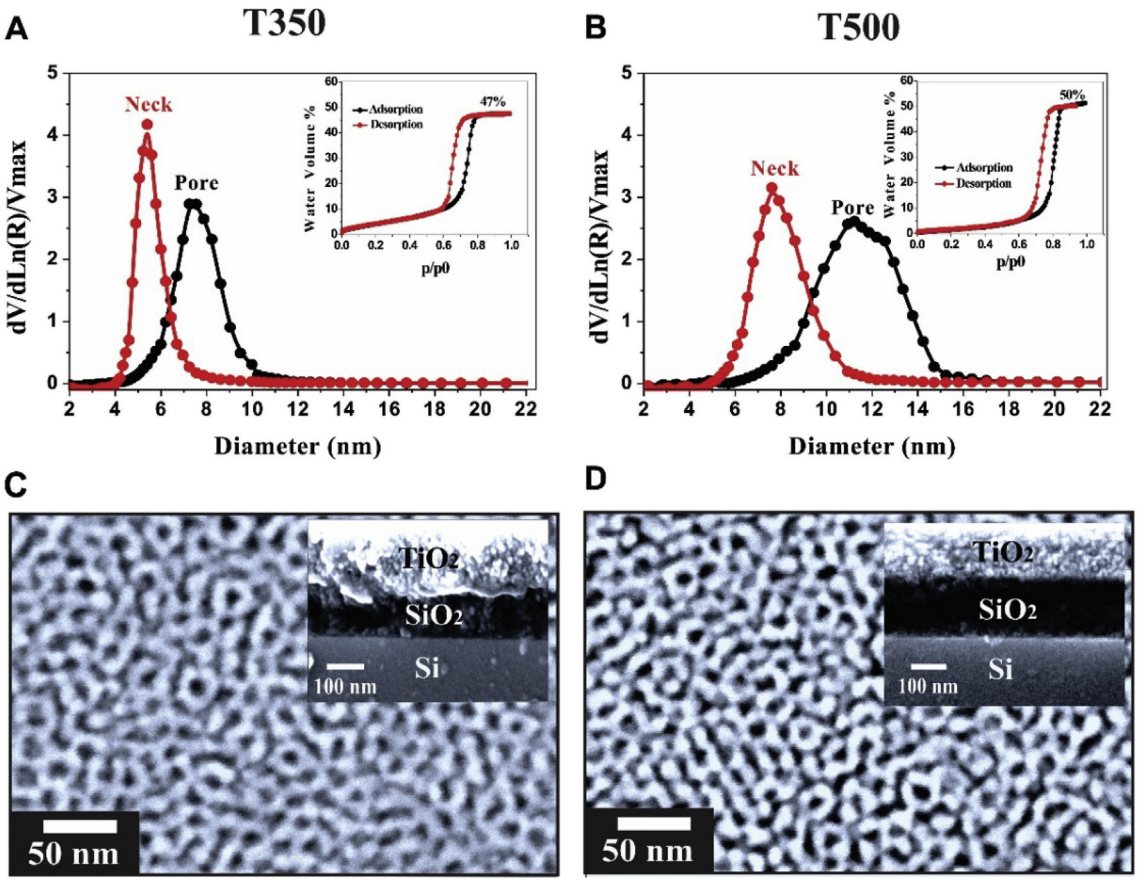


**Fig. 1.** Pore-size distribution and water adsorption–desorption isotherms insets (A and B), and FE-SEM images (C and D), of the titania thin films: T350 (left frame), and TF-500 (right frame). The inset in (C and D) depicts a cross-section view of the multilayer films.

group of samples were incubated with 0.01, 0.1 or 1 mM 1-Octanethiol (Sigma-Aldrich, St. Louis, MO) in absolute ethanol for 15 min under constant nitrogen flow to allow modification of photodeposited silver nanoparticles.

### *2.3. Fabrication of measurement device*

Two contacts (100-nm Cu layer on 10-nm Ti) were fabricated using a physical mask via a sputtering process (ATC Orion, AJA International, Inc., N Scituate, MA) on top of the mesoporous titania layer and overlapping the silver nanoparticles deposited areas at the ends parallel to the mesoporous silica ridges. Samples were stored in a desiccator and protected from light until electrical measurements were performed.

### *2.4. Characterization of mesoporous composite systems*

Scanning electron microscopy (SEM) images of mesoporous systems were obtained using a Carl Zeiss NTS Supra 40 electron microscope (Cambridge, UK). Film thicknesses, porosities and pore size distribution values were obtained from environmental ellipsometric porosimetry (EEP) (SOPRA GES5A; SOPRA, Inc.; Palo Alto, CA). Pore diameters were obtained from the pore size distribution function using a Kelvin model with a precision of ±0.5 nm using Winelli III software (SOPRA). Mesoporous titania crystalline structure was analyze by Grazing Incidence X-ray Diffraction (GIXD) using a PANalytical Empyrean diffractometer (Almelo, The Netherlands). The analysis of titania anatase phase and of silver nanoparticles

**Table 1**
Structural Data of the resulting mesoporous films.

| Sample | Neck size (nm) | Pore size (nm) | Volume (%) | Thickness (nm) | Ag:Ti |
|---|---|---|---|---|---|
| T350 | 5.4 | 7.5 | 47 | 225 | 0.3:1 |
| T500 | 7.6 | 11.2 | 50 | 230 | 0.5:1 |

Please cite this article in press as: D.C. Delgado et al., Mesoporous thin film structures as metal nanoparticle reactors for electronic circuits: Effects of matrix crystallinity and nanoparticle functionalization, Superlattices and Microstructures (2017), http://dx.doi.org/10.1016/j.spmi.2017.05.002

modification with 1-Octanethiol were performed by Raman spectroscopy using a LabRAM HR (Horiba Jobin Yvon, Kyoto, Japan).

Estimation of silver content within mesoporous composite systems was determined by calculation of Ag:Ti mass fractions using quantitative energy-dispersive X-ray spectroscopy (EDS) microanalysis in scanning electron microscopy (SEM, Quanta 200, FEI, Hillsboro, OR). To further analyze silver nanoparticles localization within the mesoporous system, X-ray photoelectron spectroscopy (XPS) was performed using a PHI 5000 VersaProbe II (Physical Electronics, Chanhassen, MN). Concentration profiles were taken by assaying ion ablation at 3 min intervals. The analysis of the results was performed using the Shirley model of background reduction. Optical properties of unmodified and thiol-modified embedded silver nanoparticles on MOTF systems deposited on glass substrate pieces were analyzed by UV−Vis spectroscopy employing a UV-1800 Shimadzu UV-VIS spectrophotometer.

The electrical characterization of the systems were performed at room temperature using a SMU Keithley 2612A (Cleveland, OH) measuring current vs. voltage (I-V) curves in the range of 0 V–2 V.

## 3. Results and discussion

The evaporation induced self-assembly (EISA) method was used to build uniform titania films with highly porous structures. The step-by-step synthesis of EISA multilayers offers the possibility to control the film porosity and composition [20,21]. Depending on the final thermal treatments (350 °C or 500 °C), the transparent and crack-free films exhibit differential development of anatase phase. These films shall hereafter be labeled T500 and T350, the tags denoting their thermal treatments. Typical $H_2O$-adsorption isotherms and pore size distributions of mesoporous films measured by EEP are shown in Fig. 1A and B. A large pore volume and controlled pore and neck sizes (estimated from the adsorption branch) were observed,

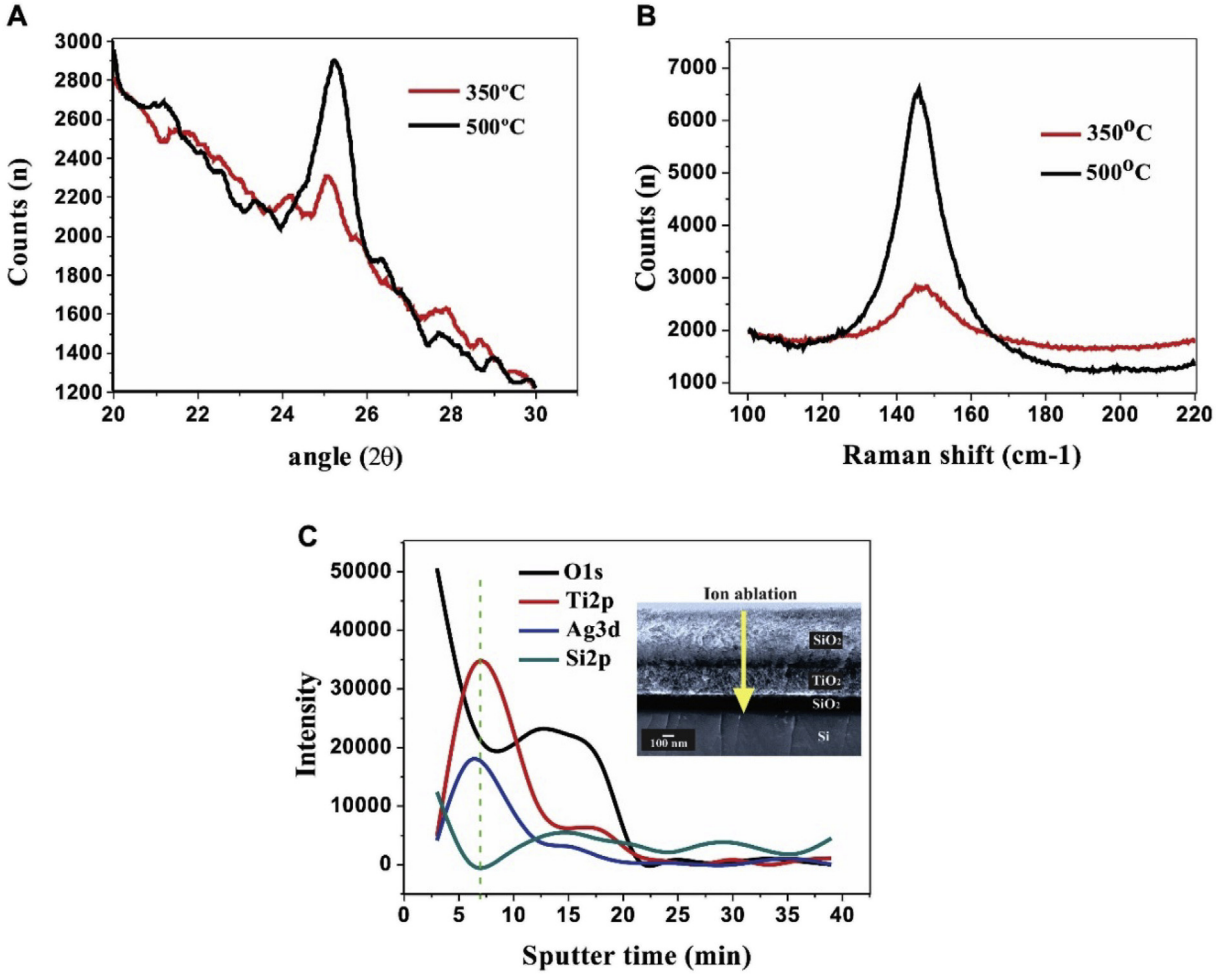


**Fig. 2.** X-ray diffraction (XRD) patterns (A) and Raman spectra (B) of T350 (red line) and T500 (black line) samples. C) XPS depth profile of the layered AgNP-T350 nanostructure. (For interpretation of the references to colour in this figure legend, the reader is referred to the web version of this article.)

Please cite this article in press as: D.C. Delgado et al., Mesoporous thin film structures as metal nanoparticle reactors for electronic circuits: Effects of matrix crystallinity and nanoparticle functionalization, Superlattices and Microstructures (2017), http://dx.doi.org/10.1016/j.spmi.2017.05.002

where greater pore dimensions were obtained in the case of T500. Pore dimensions obtained by EEP were in excellent agreement with electronic microscopy. Fig. 1C and D shows the nanoporous structure of the set of thus-prepared titania films and the morphological characteristics of these films are summarized in Table 1, indicating that film thickness ranges between 225 and 230 nm. They depict the homogeneous large-pore local order structure obtained.

In the calcination temperature range explored, contrary to T350, T500 matrix showed intense and higher X-ray diffraction peak at 25.27° (Fig. 2A) and Raman shift at 144 cm-1 (Fig. 2B), both of which are characteristic of anatase phase [22]. These demonstrated that a more extensive anatase fraction is present in T500 than in T350. A 140 nm thick intermediate layer of mesoporous $SiO_2$ with 8.5 nm diameter pores (see SI Fig. S1) was first deposited with the future purpose of electrically isolating the $TiO_2$ layer from the silicon substrate [16]. By adequately exploiting selective localization of silver nanoparticles,

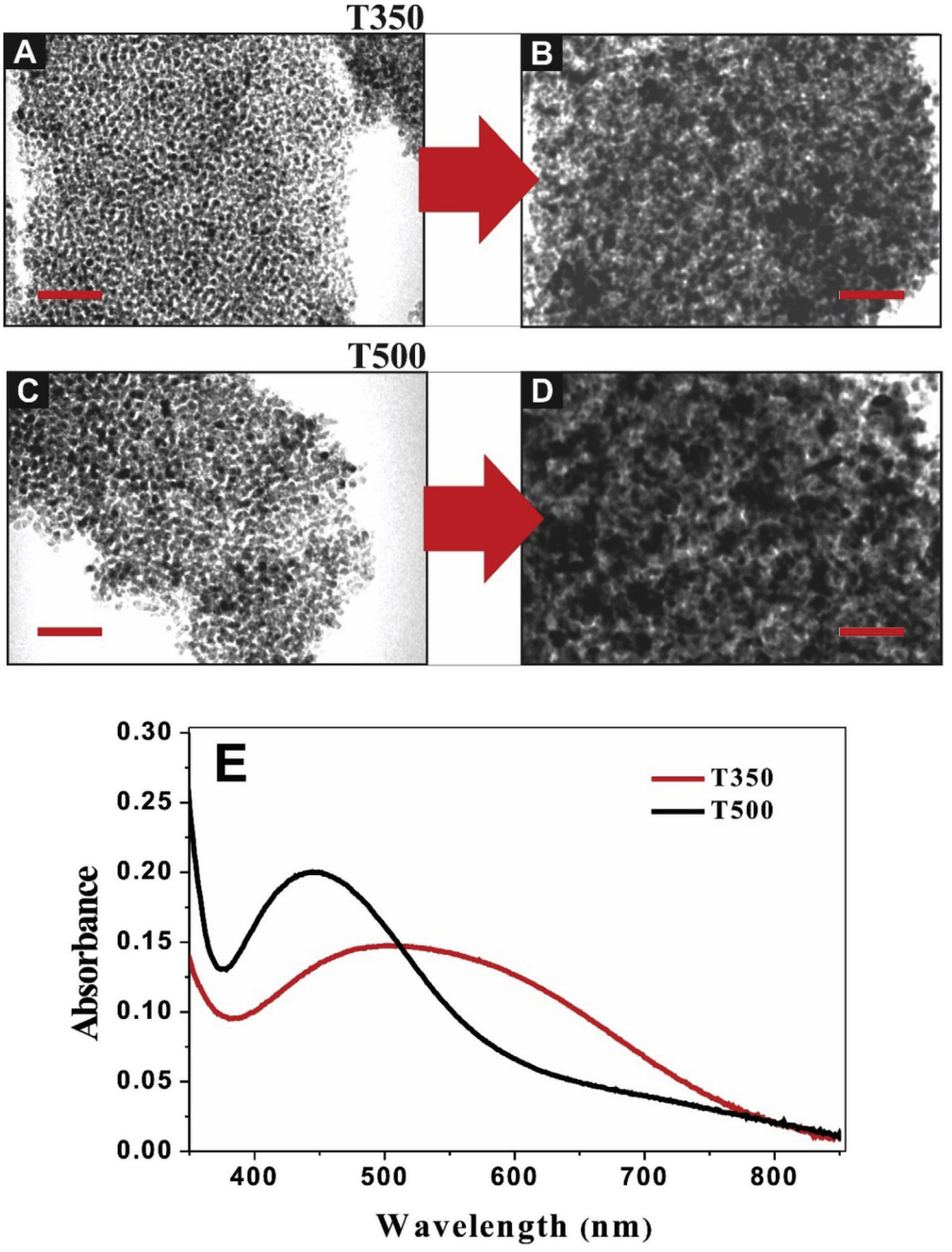


**Fig. 3.** TEM images of T350 and T500 films before (A and C) and after (B and D) infiltration with Ag nanoparticles (AgNP). Scale bare = 100 nm. E) Typical UV–vis spectra of the infiltrated T350 and T500 films.

Please cite this article in press as: D.C. Delgado et al., Mesoporous thin film structures as metal nanoparticle reactors for electronic circuits: Effects of matrix crystallinity and nanoparticle functionalization, Superlattices and Microstructures (2017), http://dx.doi.org/10.1016/j.spmi.2017.05.002

these titania pore frameworks provide an organized array of interconnected nanoreactors for nanoparticle synthesis [6,7]. Silver nanoparticles were then selectively deposited in the mesoporous titania layer by in situ photoreduction of silver ions over a square area of 6.3 $mm^2$. Fig. 2C shows that similar XPS-concentration profiles patterns after ion ablation for Ag and Ti were obtained, which in turn were different from those corresponding to the other elements. Therefore, there is a confirmed preferential Ag synthesis within the titania layer. TEM images (Fig. 3) show micrographs of Ag nanoparticles homogeneously distributed inside both titania matrices, where relatively high Ag particle loading is observed. Ag nanoparticles are 8–10 nm in diameter, which is in good agreement with the known pore dimensions of the Pluronics F127 template. Furthermore, EDS results demonstrate that Ag loading increases remarkably for the T500 samples (See Table 1).

We then performed electrical conductivity experiments to prove the potential of these nanolayer platforms. Two-terminal electrical measurements were made on all silver-titania patterned composite (Fig. 4A). The resultant I–V curve on T350 sample is displayed in Fig. 4C. Although the synthesis conditions were designed to generate silver structures formed into titania mesopores, owing to the photocatalitic character of the surface, we expected to (and did) observe a degree of coverage of the mesoporous titania surface by silver nanoparticles aggregates as well. On analysis by SEM, indeed, we observed silver paths on the surface (Fig. 4B). In order to avoid a continuous layer deposition of silver particles over the mesoporous titania surface a second mesoporous silica layer shaped like ridge was deposited by micromolding in capillaries (MIMIC, see Experimental Section) on top so to be located across the central zone of the area where nanoparticles would be deposited (Fig. 5A and B), functioning as a barrier forcing electrons to be conducted through the confined nanoparticle array within the mesoporous titania matrix (Fig. 5C). In fact, compared with the absence of the mesoporous silica barrier, the current was an order of magnitude reduced when the mesoporous ridge was present, thus confirming barrier effectiveness in interrupting electron transport through silver particles deposited on the surface of the mesoporous titania layer. Therefore, hereafter be deposited a silica mesoporous barrier on the surface of all mesoporous titania structures. Fig. 5D shows the resultant I–V curves. The I-V curves are nonlinear, approaching zero voltage a zero-current plateau develops and at a higher bias the wire becomes conductive. A source of nonlinearity might be inter-nanoparticle resistance due to silver corrosion. The shape of the I–V curve could then be attributed to electrochemical processes in the corrosion barriers [23]. The red line depicts that currents were significantly higher for matrix treated at 350 °C than for matrix treated at 500 °C. Although T500 matrix

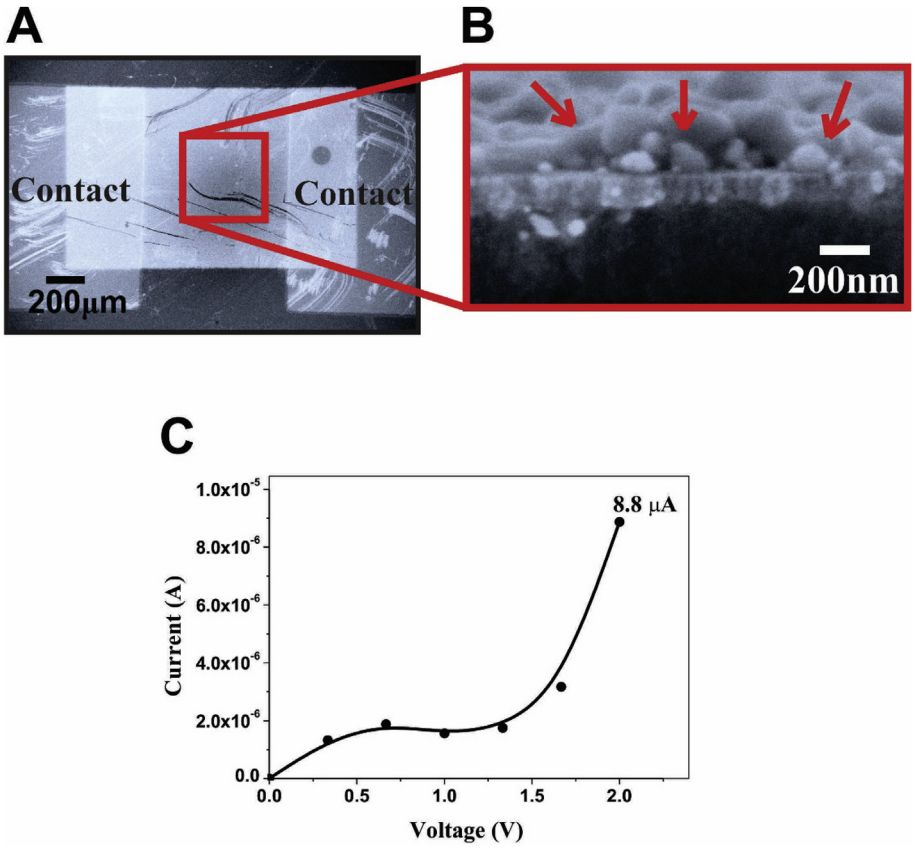


**Fig. 4.** SEM image of the T350 sample presenting a patterned square of AgNP–titania composite. B) FE-SEM cross section of the Ag infiltrated T350 films in the absence of the mesoporous silica barrier. The arrows indicate silver nanoparticles along the film surface. C) Current–voltage response curve of T350 films including silver nanoparticles without the silica barrier.

Please cite this article in press as: D.C. Delgado et al., Mesoporous thin film structures as metal nanoparticle reactors for electronic circuits: Effects of matrix crystallinity and nanoparticle functionalization, Superlattices and Microstructures (2017), http://dx.doi.org/10.1016/j.spmi.2017.05.002

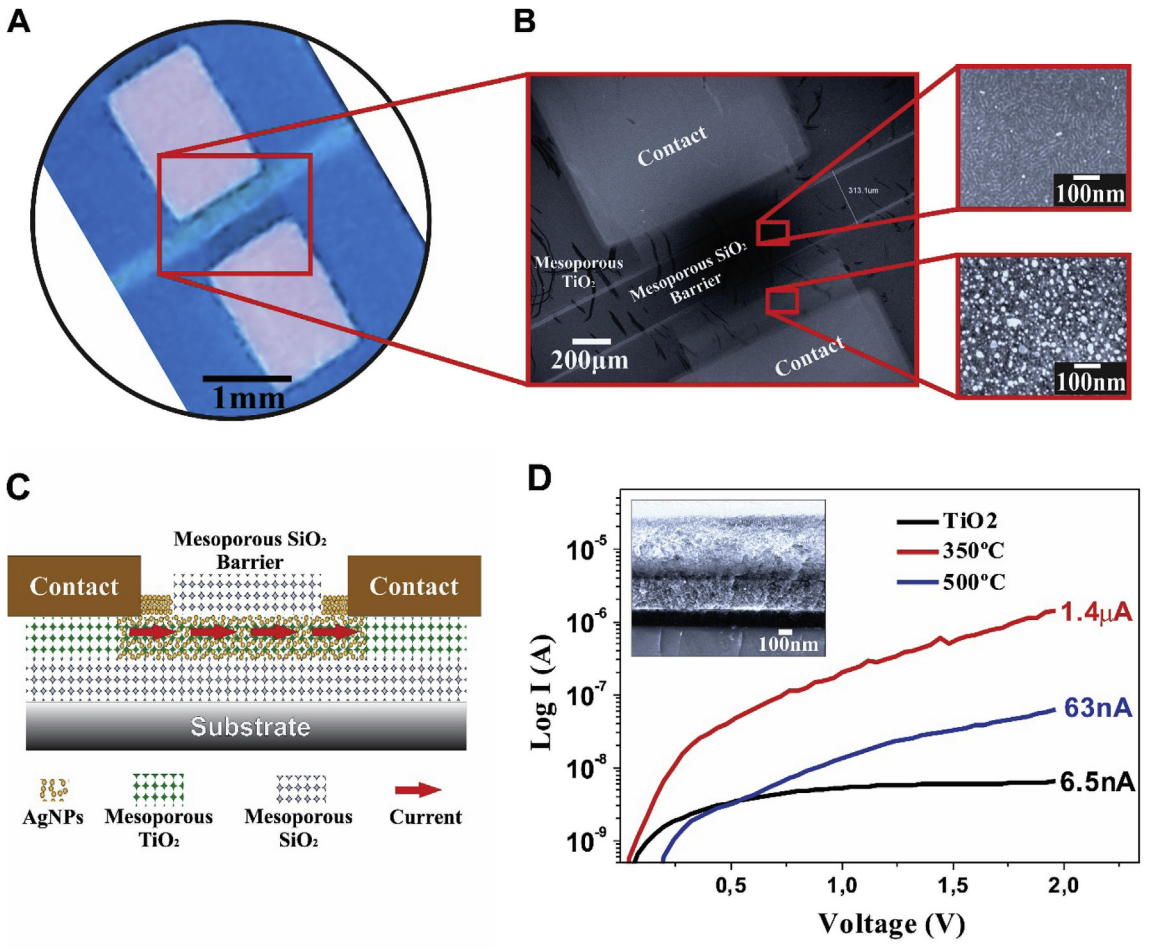


**Fig. 5.** (A) Optical top-view imagen of the patterned region composed of silver nanoparticles, presenting the $SiO_2$ barrier on the titania layer. (B) SEM image of the sample shown in A. Note that no formation of silver paths in the silica barrier is observed. (C) Side scheme of the composite structure of the layered film submitted to electrical resistant measurement. (D) Log current – voltage curve of T350 (red line) and T500 (blue line) including silver nanoparticles. Inset shows SEM image of the 3-layered film where no superficial silver particles are observed. (For interpretation of the references to colour in this figure legend, the reader is referred to the web version of this article.)

showed higher silver content than T350 matrix (Table 1), the T350 higher current value is not surprising owing to the expected interactions, from optical analysis, among silver nanoparticles in the T350 system. The position of plasmon absorption bands can be interpreted in terms of silver particle interactions [24,25]. Coincidently, a red shift in the silver plasmon resonance is observed in the T350 samples due to interparticle coupling (Fig. 3C) [24,25].

The stability of the nanocomposite structure, and hence the reproducibility of electrical system was evaluated by periodically measuring current response and plasmon resonance of embedded silver nanoparticles. To test the electrical stability of the system we ran the titania hosting silver nanoparticles for repeated voltage cycles from 0 to 2 V. Fig. 6A provides a measure of current at 2 V ($I_{2v}$) of the T350 against cycle number, showing that $I_{2v}$ dropped very significantly after 3 cycles. The stability of nano-electronic platforms is crucial for practical applications. Considering this point, the stability of the system was enhanced through upon chemisorption of organosulfur compounds SAMs [26]. Effective functionalization of silver nanoparticle array with 1-octanethiol was demonstrated by Raman spectroscopy (Fig. 6B), showing the disappearance of the 2580 $cm^{-1}$ shift characteristic of the S-H bond through formation of the S-Ag bond in the functionalized nanoparticle arrays [27,28]. The nanoparticle array stability was evaluated by periodically measuring plasmon resonance storing the samples at room temperature for a given time and performing new plasmon measurements. Plasmon resonance measurements give an overall idea of silver nanoparticle array structure and interaction [24,25]. After a slight initial decrease during the first day, maximum plasmon absorbance maintained more than 98% of its initial value after storage for 15 days (Fig. 6C). A significant unstable period can however be noted for the non-functionalized nanoparticle arrays. This illustrates the good stability of the thiol-modified nanoparticle system. Yet more importantly, the electrical stability of these functionalized silver loaded mesoporous films did not deteriorate on repeated use. Fig. 6A shows that the current remains fairly stable up to 20 voltage cycles. The origin of the slight lower conductivity observed in the functionalized system could be due to a thiol blockade

Please cite this article in press as: D.C. Delgado et al., Mesoporous thin film structures as metal nanoparticle reactors for electronic circuits: Effects of matrix crystallinity and nanoparticle functionalization, Superlattices and Microstructures (2017), http://dx.doi.org/10.1016/j.spmi.2017.05.002

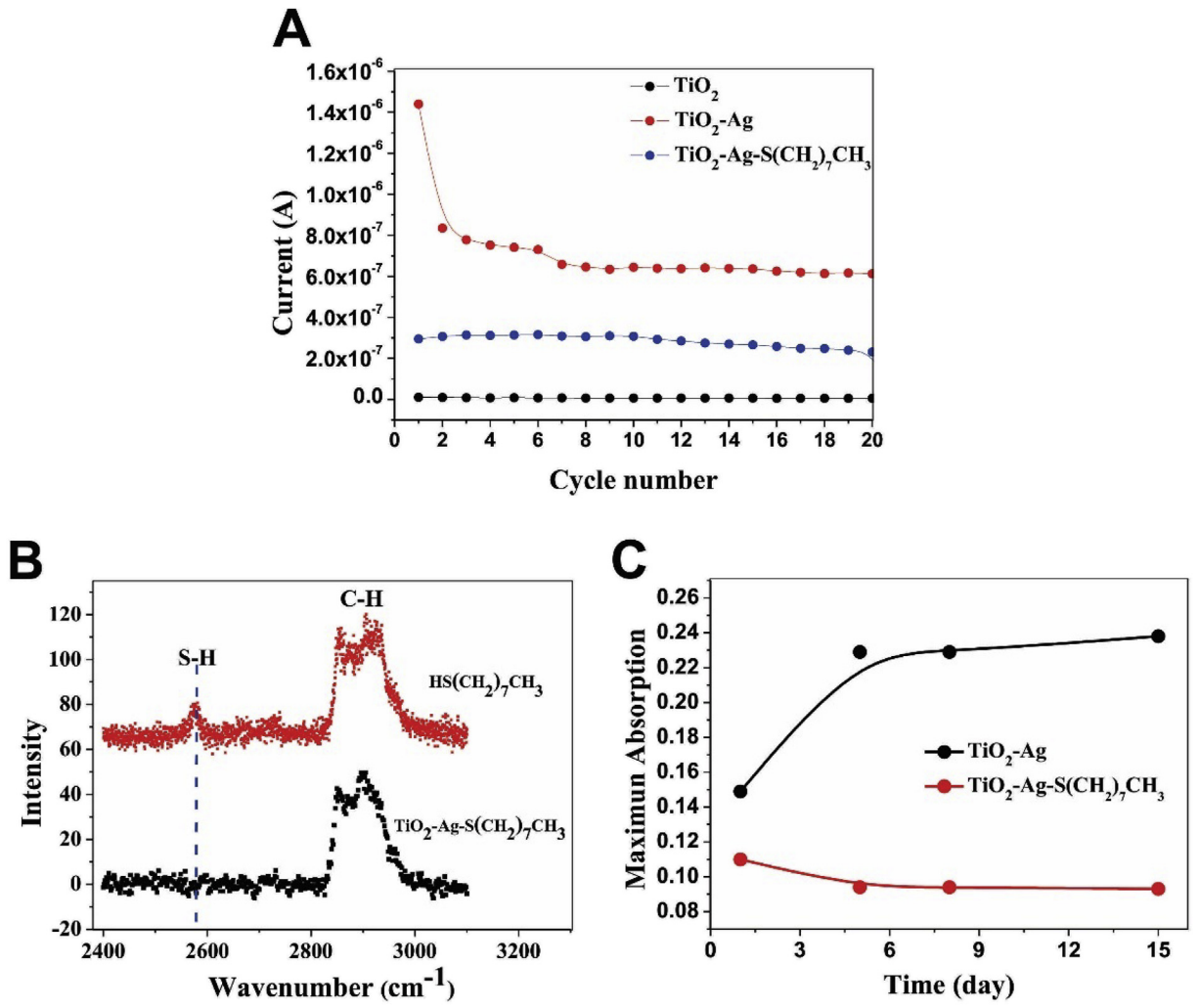


**Fig. 6.** A) The current at 2 V versus cycle number for T350 matrix (black dots), AgNP-T350 composites (red dots) and functionalized AgNP-T350 samples (blue dots). B) Ag-S$(CH_2)_7CH_3$ raman signal in functionalized nanoparticles (black dots). 1-octanethiol raman signal is shown for comparison (red dots). C) Long-term variation of the absorbance at the plasmon peak maximum for no-modified (black) and thiol-functionalized silver nanoparticles (red) into mesoporous films. (For interpretation of the references to colour in this figure legend, the reader is referred to the web version of this article.)

phenomenon. These results are nonetheless a clear step to integrate these nanocomposite structures for practical applications, such as biosensing devices, where good system stability is essential. Although others have reported sol-gel based silver nanoparticle composites [5,10,29] these are the first mesoporous platforms in which accessible, stabilized and electrically conductor metal nanoparticle arrays can be clearly obtained, paving the way for creating novel electronic sensors.

## 4. Conclusions

In summary, our results demonstrate that MOTF can be applied to the rational design and synthesis of metal nanostructures, exhibiting improved performance in electronic properties such as stability and directional currents. For the former, we have delineated SAMs functionalization that control the stability of nanoparticle-based structures, and for the latter, we have shown that a barrier of mesoporous silica on titania film impart localized currents along the embedded silver nanoparticles. The synergy between electrical stability, current confinement, accessibility of the mesopore system, thin film architecture and compatibility with microelectronic microfabrication processes together with simplicity and low cost of the system presented here is a promising step toward mesoporous material applications in practical devices. It is worth mentioning that the assembly system is also modular, and can therefore be extended to numerous SAMs functionalization giving rise to a novel generation of biofunctional devices in many exciting areas of current research, which ranges a variety of applications. Among the interesting capabilities derived from these helpful features, we can mention the protective

Please cite this article in press as: D.C. Delgado et al., Mesoporous thin film structures as metal nanoparticle reactors for electronic circuits: Effects of matrix crystallinity and nanoparticle functionalization, Superlattices and Microstructures (2017), http://dx.doi.org/10.1016/j.spmi.2017.05.002

properties of the mesoporous matrix on metal nanoparticles in extreme environment conditions, or the possibility of size controlling molecule access along the pore matrix to enhance the system selectivity. Although silver and titania nanowires have been used for developing electronic sensors [30,31], the versatile features aforementioned of Ag/titania nanostructured platform here presented create additional opportunities for building up new sensor devices. An especially appealing area of application is in cheap/disposable sensors including biosensors. Looking forward, we envision our meso/Ag nanoparticle circuitry being biofunctionalized from thiolate ligands incorporating DNA for distinguishing specific target sequences due to hybridization-based changes in the conductivity of the silver nanoparticle circuit.

## Acknowledgment

DCD acknowledges their doctoral fellowships from CONICET, Argentina. Andres Di Donato is acknowledged for helping with electrical measurements and for inspiring discussions. This work was supported by ANPCyT (PICT-2013-1490 and PICT-2012-2969), Argentina.

## Appendix A. Supplementary data

Supplementary data related to this article can be found at http://dx.doi.org/10.1016/j.spmi.2017.05.002.

## References

[1] K. Tapio, J. Leppiniemi, B. Shen, V.P. Hytönen, W. Fritzsche, J.J. Toppari, Toward single electron nanoelectronics using self-assembled DNA structure, Nano Lett. 16 (2016) 6780–6786.
[2] G. Presnova, D. Presnov, V. Krupenin, V. Grigorenko, A. Trifonov, I. Andreeva, O. Ignatenko, A. Egorov, M. Rubtsova, Biosensor based on a silicon nanowire field-effect transistor functionalized by gold nanoparticles for the highly sensitive determination of prostate specific antigen, Biosens. Bioelectron. 88 (2017) 283–289.
[3] J. Zhu, M.C. Hersam, Assembly and electronic applications of colloidal nanomaterials, Adv. Mater. 29 (2017) 1603895.
[4] G.T. Chandran, X. Li, A. Ogata, R.M. Penner, Electrically transduced sensors based on nanomaterials (2012–2016), Anal. Chem. 89 (2016) 249–275.
[5] J. Corde, S. Perruchas, L. Vieille, J.-P. Galaup, S. Duluard, C. Biver, J.-P. Boilot, T. Gacoin, Photolithographic processing of silver loaded dielectric coatings based on preformed colloidal TiO2 nanoparticles dispersed in a mesoporous silica binder, Nanotechnology 23 (2012) 505206.
[6] E.D. Martiínez, M.G. Bellino, G.J.A.A. Soler-Illia, Patterned production of silver-mesoporous titania nanocomposite thin films using lithography-assisted metal reduction, ACS Appl. Mater. Interfaces 1 (2009) 746–749.
[7] J. Ginter, A. Kisielewska, K. Spilarewicz-Stanek, M. Cichomski, D. Batory, I. Piwoński, Tuning of the photocatalytic activity of thin titanium dioxide coatings by highly ordered structure and silver nanoparticles, Microporous Mesoporous Mater 225 (2016) 580–589.
[8] M.C. Fuertes, M. Marchena, M.C. Marchi, A. Wolosiuk, G.J.A.A. Soler-Illia, Controlled deposition of silver nanoparticles in mesoporous single- or multilayer thin films: from tuned pore filling to selective spatial location of nanometric objects, Small 5 (2009) 272–280.
[9] D.S. Likius, H. Nagai, S. Aoyama, C. Mochizuki, H. Hara, N. Baba, M. Sato, Percolation threshold for electrical resistivity of Ag-nanoparticle/titania composite thin films fabricated using molecular precursor method, J. Mater. Sci. 47 (2012) 3890–3899.
[10] S.Y. Jung, T.J. Ha, C.S. Park, W.S. Seo, Y.S. Lim, S. Shin, H.H. Cho, H.H. Park, Improvement in the conductivity ratio of ordered mesoporous Ag-TiO 2 thin films for thermoelectric materials, Thin Solid Films 529 (2013) 94–97.
[11] J.C. Love, L.A. Estroff, J.K. Kriebel, R.G. Nuzzo, G.M. Whitesides, Self-assembled Monolayers of Thiolates on Metals as a Form of Nanotechnology, 2005.
[12] S. Zeng, K.-T. Yong, I. Roy, X.-Q. Dinh, X. Yu, F. Luan, AuNP138-A review on functionalized gold nanoparticles for biosensing applications, Plasmonics 6 (2011) 491–506.
[13] P.C. Angelomé, L.M. Liz-Marzán, Synthesis and applications of mesoporous nanocomposites containing metal nanoparticles, J. Sol-Gel Sci. Technol. 70 (2014) 180–190.
[14] A. Wolosiuk, N.G. Tognalli, E.D. Martínez, M. Granada, M.C. Fuertes, H. Troiani, S.A. Bilmes, A. Fainstein, G.J.A.A. Soler-Illia, Silver nanoparticle-mesoporous oxide nanocomposite thin films: a platform for spatially homogeneous SERS-active substrates with enhanced stability, ACS Appl. Mater. Interfaces 6 (2014) 5263–5272.
[15] H. Nourolahi, A. Behjat, S.M.M. Hosseini Zarch, M.A. Bolorizadeh, Silver nanoparticle plasmonic effects on hole-transport material-free mesoporous heterojunction perovskite solar cells, Sol. Energy 139 (2016) 475–483.
[16] E.D. Martínez, L. Granja, M.G. Bellino, G.J.A.A. Soler-Illia, Electrical conductivity in patterned silver–mesoporous titania nanocomposite thin films: towards robust 3D nano-electrodes, Phys. Chem. Chem. Phys. 12 (2010) 14445.
[17] E. Kim, Y. Xia, G.M. Whitesides, Micromolding in capillaries: applications in materials science, J. Am. Chem. Soc. 1185722 (1996) 5722–5731.
[18] B. Rühle, M. Davies, T. Lebold, C. Bräuchle, T. Bein, Highly oriented mesoporous silica channels synthesized in microgrooves and visualized with single-molecule diffusion, ACS Nano 6 (2012) 1948–1960.
[19] Y. Xia, G.M. Whitesides, Soft lithography, Angew. Chem. Int. Ed. 37 (1998) 550–575.
[20] J.C. Brinker, Y. Lu, A. Sellinger, H. Fan, Evaporation-induced self-assembly: nanostructures made easy, Adv. Mater 11 (1999) 579–585.
[21] L. Mahoney, R.T. Koodali, Versatility of Evaporation-Induced Self-Assembly (EISA) method for preparation of mesoporous TiO2 for energy and environmental applications, Mater. (Basel) 7 (2014) 2697–2746.
[22] J. Hugman, B.S. Richards, A. Crosky, Phase characterisation of TiO2 thin FIlms using micro-raman spectroscopy and glancing angle x-ray diffraction, IEEE (2002) 181–184.
[23] Z. Ebrahimpour, N. Mansour, Annealing effects on electrical behavior of gold nanoparticle film: conversion of ohmic to non-ohmic conductivity, Appl. Surf. Sci. 394 (2017) 240–247.
[24] L. Zhao, L.L. Zhao, K.L. Kelly, K.L. Kelly, G.C. Schatz, G.C. Schatz, The extinction spectra of silver nanoparticle arrays: influence of array structure on plasmon resonance wavelength and width, J. Phys. Chem. B 107 (2003) 7343–7350.
[25] N.J. Halas, S. Lal, W.S. Chang, S. Link, P. Nordlander, Plasmons in strongly coupled metallic nanostructures, Chem. Rev. 111 (2011) 3913–3961.
[26] M. Himmelhaus, F. Eisert, M. Buck, M. Grunze, Self-assembly of n-alkanethiol monolayers. A study by IR-visible sum frequency spectroscopy (SFG), J. Phys. Chem. B 104 (2000) 576–584.
[27] M.A. Bryant, J.E. Pemberton, Chemical 11 (1991).
[28] Y. Li, O. Zaluzhna, B. Xu, Y. Gao, J.M. Modest, Y.J. Tong, Mechanistic insights into the Brust-Schiffrin two-phase synthesis of organo-chalcogenate-protected metal nanoparticles, J. Am. Chem. Soc. 133 (2011) 2092–2095.
[29] H. Li, G. Zhao, B. Song, G. Han, Effect of incorporation of silver on the electrical properties of sol-gel-derived titania film, J. Clust. Sci. 19 (2008) 667–673.

Please cite this article in press as: D.C. Delgado et al., Mesoporous thin film structures as metal nanoparticle reactors for electronic circuits: Effects of matrix crystallinity and nanoparticle functionalization, Superlattices and Microstructures (2017), http://dx.doi.org/10.1016/j.spmi.2017.05.002

[30] V.A. Online, W.R. Small, V.N. Paunov, Dielectrophoretic Fabrication of Electrically Anisotropic Hydrogels with Bio-functionalised Silver Nanowires, 2013, pp. 5798–5805.
[31] K.C. Hwang, Chung-Hsuan Wu, Wei-Han Wang, Chien-Chong Hong, A disposable breath sensing tube with on-tube single-nanowire sensor array for on-site detection of exhaled breath biomarkers, Lab. Chip 16 (2016) 4395–4405.

Please cite this article in press as: D.C. Delgado et al., Mesoporous thin film structures as metal nanoparticle reactors for electronic circuits: Effects of matrix crystallinity and nanoparticle functionalization, Superlattices and Microstructures (2017), http://dx.doi.org/10.1016/j.spmi.2017.05.002